Nuclear Materials and Energy 12 (2017) 193–199

Contents lists available at ScienceDirect

Nuclear Materials and Energy

journal homepage: www.elsevier.com/locate/nme

The high field side high density region in SOLPS-modeling of nitrogen-seeded H-modes in ASDEX Upgrade

F. Reimold[a,*], M. Wischmeier[a], S. Potzel[a], L. Guimarais[c], D. Reiter[b], M. Bernert[a], M. Dunne[a], T. Lunt[a], the ASDEX Upgrade team[a], the EUROfusion MST1 team[1]

[a] Max-Planck-Institut für Plasmaphysik, Boltzmannstraße 2, D-85748 Garching, Germany
[b] Institut für Energie- und Klimaforschung - Plasmaphysik, Forschungszentrum Jülich GmbH, Germany
[c] Instituto de Plasmas e Fusão Nuclear, Universidade de Lisboa, Portugal

ARTICLE INFO

Article history:
Received 6 July 2016
Revised 5 December 2016
Accepted 5 January 2017
Available online 9 March 2017

Keywords:
PSI-21: Edge modeling
Divertor plasma
ASDEX-Upgrade
Detachment
High field side high density
SOLPS

ABSTRACT

The understanding of divertor physics and the evolution of divertor detachment is crucial for developing the capability to model power exhaust in current experiments and reliably predict it for future fusion devices. In simulations of ASDEX Upgrade, an experimentally observed region of high density in the high field side scrape-off layer has been recovered. Validated modeling with SOLPS5.0 shows that a detailed match of the high field side scrape-off layer plasma is not only important for local plasma parameters, but can lead to strong changes in global parameters. Drifts play a crucial role in lower-single null discharges with forward toroidal field ($\nabla\vec{B}$-drift pointing down). Their inclusion changes the spatial extent as well as the radial and poloidal gradients of the high field side high density. Adapted transport coefficients that take into account core fueling by plasma diffusion due to the presence of the high field side density and drift-driven radial fluxes now reconcile the modeled deuterium compression ratio, divertor neutral density, neutral radiation levels and deuterium fueling rates with experimental measurements. The onset of strong volume recombination in the simulations now allows to remove the previously necessary increase of perpendicular transport in the inner divertor from the simulations.

1. Introduction

Future fusion devices like ITER [1] and DEMO [2] will have to be operated with a detached divertor to meet material limits, which are otherwise largely exceeded at the divertor targets [3,4]. A sound understanding of the controlling physics in the divertor and scrape-off layer plasma as well as of the interplay of the individual processes in the evolution of divertor detachment is crucial for developing the capability to accurately model power exhaust experiments in current devices such as ASDEX Upgrade or JET [5,6] and ultimately develop a predictive capability for future fusion devices, such as ITER or DEMO. Previous numerical modeling with SOLPS5.0 has shown that most experimental measurements can be reproduced in the fluctuating [7] and completely detached plasma scenarios as in nitrogen-seeded ASDEX Upgrade H-Modes [5,8]. However, the neutral density and compression in the (sub-)divertor could not be reproduced using the experimental upstream profiles [8]. The persistent discrepancy with experiment manifested in the simulations via an underprediction of the neutral flux densities, the line-integrated Balmer line intensities (D_δ & D_ϵ) and the deuterium fueling rates. In addition, almost no volume recombination occurred in these simulations despite experimental indications of recombining plasma in the inner divertor [9].

This paper presents new SOLPS5.0[2] modeling, which shows that it can be crucial to match the experimental measurements in *both* divertors accurately – as opposed to matching the outer divertor only – in order to obtain an improved plasma solution.

It has been shown experimentally that a region of high density in the high field side scrape-off layer – the so-called high field side high density (HFSHD) – is connected to the evolution of the divertor towards complete detachment and to the fueling of the core plasma [5,7,10,11]. Such a high density region also forms in our simulations of the fluctuating detachment state, where it plays

* Corresponding author.
E-mail address: f.reimold@fz-juelich.de (F. Reimold).
[1] see http://www.euro-fusionscipub.org/mst1.

[2] Modified SVN Revision 4551 at http://solps-mdsplus.aug.ipp.mpg.de/repos/SOLPS/trunk/solps5.0/ (restriced access).

http://dx.doi.org/10.1016/j.nme.2017.01.010

an important role in the fueling of the core plasma and largely determines the achievable neutral pressure in the divertor for a given upstream separatrix density. Consistent with experimental data, the high density region forms with sufficient heating power [7,12] and extends out of the divertor up to the inner midplane [11]. The nature of the core plasma fueling is changed – with potential implications for plasma performance [12,13] – and is at least partly responsible for the previous discrepancies of modeling and experiment in the particle throughput and divertor neutral density. An improved match of the high field side scrape-off layer plasma and the analysis of its dynamics enables us to match the experimental neutral compression, fueling rates and to obtain a significant recombination sink for ions in the inner divertor, while maintaining comparable agreement with the other experimental measurements as previous modeling [8].

The experimental setup of the modeled H-mode experiments is shortly presented in Section 2. The modeling setup is detailed in Section 3. The impact of the high field side high density on the simulations and of input parameters on the high field side high densityis discussed in Section 4. A discussion and summary in Section 5 closes the paper.

2. The experimental setup

The selected ASDEX Upgrade H-mode discharge (#28903) was a lower single null configuration with a plasma current of $I_P = 800$kA, a toroidal field of $B_t = 2.5$T ($\nabla\vec{B}$-drift points down) and a total heating power of $P_H = 8.2$MW. The separatrix electron density at the outer midplane is about $n_e = 2.5 \times 10^{19}\mathrm{m}^{-3}$ with a central line integrated density of $\langle n_e \rangle = 6.8 \times 10^{19}\mathrm{m}^{-3}$. Measured core plasma impurity concentrations were about $c_N = 0.5\%$, $c_C \approx 0.1\%$, $c_{He} \approx 0.5\%$ in the modeled, non-seeded reference phase. The tungsten core concentration varied between $c_W = 1.5 - 3.0 \times 10^{-5}$. The discharge #28903 is modeled for an averaged inter-ELM period in the time slice from 2.0 – 2.6s. ELM-synchronization has been used to restrict experimental data to stable inter-ELM phases where possible. The plasma is in the fluctuating detachment state [7], where the impact of the high field side high density is most pronounced. This state features a detached inner divertor and an outer divertor in the high-recycling regime. The discharge is described in more details in Refs. [5,8].

3. The modeling setup

The SOLPS5.0 code package [14] has been used for the modeling. SOLPS mainly consists of two coupled codes: B2.5 [15] is a fluid code that solves Braginskii-like equations for ions (D, C, He, N) and electrons. Eirene is a Monte-Carlo code that describes kinetic neutrals [16]. Both codes are coupled via source terms and are called iteratively. The reference equilibrium for the grid generation is taken at 2.4s of the discharge #28903. The separatrix density is set by a neutral gas puff of deuterium molecules at the experimental feed-forward fueling rate of 2.0×10^{22} $\mathrm{e}^{-}\mathrm{s}^{-1}$. A puff of nitrogen atoms at a low seeding rate ($\sim 10^{19}$ $\mathrm{e}^{-}\mathrm{s}^{-1}$) is applied to account for residual wall sources of nitrogen from seeding in the previous discharges. The densities of fully-stripped helium and carbon ions are set to fixed values at the core boundary to match the experimental core impurity concentrations. Deuterium, helium and nitrogen are assumed to be fully recycling, whereas carbon is assumed to be a sticking species. The input power into the simulation domain takes into account the core radiation – predominantly from tungsten. The latter is determined from bolometric tomography that is in accordance with power balance. The power flow across the separatrix in the simulations is 5–6 MW. A more detailed description of the input parameter settings can be found in Appendix A.

4. The high field side high density in SOLPS-modeling

In boundary plasma modeling a substantial mismatch with experimental data of the inner divertor plasma has been recognized by the plasma edge community for a long time. Despite significant effort devoted to address it, matching the inner divertor experimental data and the in/out divertor asymmetries has remained an elusive challenge for detached regimes. The situation was aggravated by a common lack of experimental data from the high field side scrape-off layer. However, these locations can be important in determining the boundary plasma solution in ASDEX UpgradeH-modes in the entire modeling domain. A key ingredient in how the high field side scrape-off layer plasma determines the plasma solution is the development of a high field side high density region.

The inner divertor receives significantly less power (inter-ELM) than the outer divertor [18,19], the baffling for neutrals is stronger and the parallel connection length as well as the flux expansion is larger. This leads to a colder and more dense plasma – with increased radiation losses – already for pure deuterium fueling. Decreased losses of impurity neutrals to the main chamber by strong baffling and plasma conditions that favor a suppression of the temperature gradient force out of the divertor as well as an increased friction drag towards the divertor plate below the X-point allow for a larger impurity retention. Higher impurity content in combination with high electron densities then additionally allow for increased radiation losses from low-Z impurities. These self-amplifying processes in the inner divertor lead to a transition to the high-recycling regime and to low target temperatures at lower upstream densities than for the outer divertor. As a consequence SOLPS simulations of ASDEX Upgradeusually exhibit a region of high density and low temperature (1–2 eV) in the inner divertor, which is initially confined to the volume between the X-point, the inner strikepoint and the divertor nose, see Fig. 1. Drifts and the transport model change the spatial extent and the magnitude of this high density. The remainder of the paper will describe how the interaction of these two drivers can lead to a better match with experiment and how this allows to increase the neutral compression in the simulations.

4.1. The role of drifts

Activating drifts in the simulations leads to additional particle fluxes from the outer divertor into the private-flux region and from there into the inner divertor [20]. This furthers the described tendency of high density and low temperature in the inner divertor and leads to a reduction of the density and a reciprocal increase of the temperature in the outer divertor. Additional redistribution of the heat flux from the inner to the outer divertor due to drifts again amplifies the effect [21]. Lower impurity retention and lower density in the outer divertor also lead to larger in-out asymmetries of the impurity concentration and to a reduction of the radiation losses in the outer divertor. For the outer/inner target all this triggers the onset of high-recycling and detachment at higher/lower upstream densities compared to simulations without drifts. Drifts also change the particle flow pattern in the divertor and close to the X-point in the common scrape-off layer [21]. In particular on the high field side, the combination of the poloidal and perpendicular $\vec{E} \times \vec{B}$-drifts lead to additional particle fluxes into the far scrape-off layer [22]. In the drift cases we analyzed, the heat flux profile was also shifted outward into the inner far scrape-off layer. The redistributed heat and particles then help to establish a 'high-recycling' regime in the high field side far scrape-off layer by increasing the ionization sources there. The high field side high density region broadens – in perpendicular and poloidal direction – and the maximum density in the inner divertor increases. The high density region extends along the inner target to above the divertor

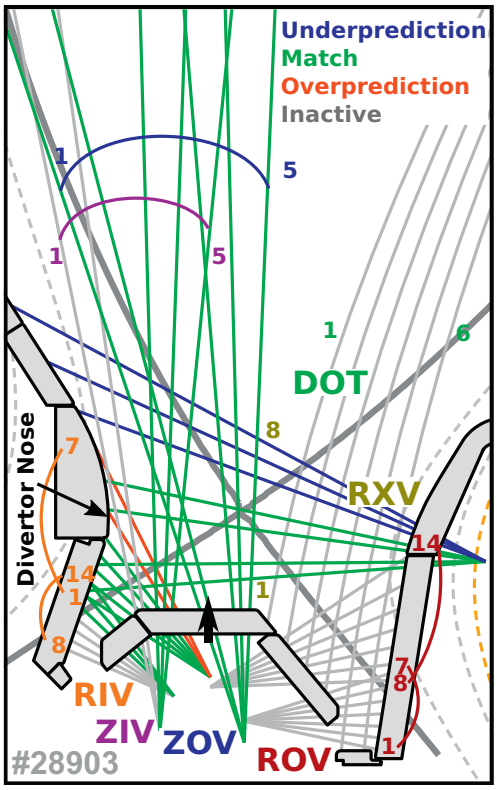

Fig. 1. The divertor spectroscopy lines of sight [7] at ASDEX Upgrade are shown along with the gray shaded region of the high field side high density. Modeled and experimental densities from Stark broadening analysis [17] are compared: green - agreement within a factor of two; blue/red - under-/overprediction of the density in the simulation. (For interpretation of the references to colour in this figure legend, the reader is referred to the web version of this article.)

nose and up to the inner midplane. With the increase of the recycling fluxes in the far scrape-off layer consequently the high field side neutral fluxes above the X-point are significantly increased.

A second order effect, that moderates the effect of this high-recycling in the high field side far scrape-off layer, can be exerted by the neutral conductances of the subdivertor structures of ASDEX Upgrade. These allow the high neutral fluxes of the inner divertor to migrate towards the main chamber and/or to equilibrate with the subdivertor pressure. Vice-versa high neutral subdivertor pressures can provide additional neutrals and help to sustain the high field side scrape-off layer recycling. This moderation effect can play a role in the numerical and physical stabilization of the simulations, but the neutral conductances alone in simulations without drifts so far have not been sufficient to establish high-recycling in the far scrape-off layer.

4.2. Role of plasma fueling

Scrutinizing the high density region in the high field side scrape-off layer, it became clear that two additional processes need to be considered for fueling of the confined plasma. Fig. 2(a) shows density profiles at the low field side (red) and high field side (green) midplane. At the inner midplane the density gradients are inverted at the separatrix. Such inverted gradients can be present in drift simulations between the X-point and the inner midplane and lead to a diffusive plasma flow across the separatrix, see red shaded region in Fig. 3. In addition, a drift-driven plasma flow across the separatrix also provides a particle source for the confined plasma, see blue shaded region in Fig. 3. The high field side high density changes the balance of the outward and inward directed drift-driven particle flows by changing the poloidal asymmetry of the plasma profiles, which in turn impacts on the ionization distribution and the flow pattern in the scrape-off layer. Analysis of the flows and their interconnection to the drift-driven fluxes will be presented elsewhere. The amount of drift-driven and diffusive particle influx can be comparable to the effective ionization source due to neutrals inside the confined plasma. Neglecting the effective particle source due to an influx of plasma in our assessment of how the confined plasma is fueled had prohibited us in the past to achieve the experimental neutral compression due to an overprediction of the separatrix densities for a given neutral pressure in the divertor.

In order to achieve the correct neutral compression in the simulations, the particle diffusion coefficients need to be reduced to low values ($D \approx 0.01 - 0.10 \frac{m^2}{s}$) in the proximity of the separatrix to decrease the fueling by inward diffusive plasma flow and to confine the high density more to the divertor. Including a perpendicular outward convective transport component in the low field side scrape-off layer to mimic the convective transport by filaments can further lower the fueling of the core by plasma influx. The reduction of the plasma flow into the confined plasma allows to increase the neutral fueling rates to experimental levels. A fixed pumping speed of the pumping system then automatically implies an increase of the neutral density in the divertor and in turn a significant increase of the neutral radiation. In contrast to previous modeling [8], the neutral divertor density and the neutral radiation are now widely consistent with experimentally observed levels. The adaptation of the transport model also included a reduction of the previously necessary additional perpendicular transport in the divertor volume [8]. The reduction of the perpendicular diffusion coefficients in the divertor back to original level results in an additional increase of the gradients and the maximum of the density in the inner divertor. This has two beneficial effects with respect to an improved match to the experiment. First, the extent of the high density region out of the divertor is reduced and the density is more strongly peaked in the vicinity of the divertor target. This reduces the plasma influx into the confined plasma further by reducing the density and its radial gradients at the high field side separatrix. Second, the increase in the peak particle density leads to the onset of strong recombination, which we will discuss in the following.

4.3. The role of recombination

In the past, we always attempted to match the low experimental values of the ion saturation current measurements at the inner target by locally increasing the divertor transport coefficients [8]. This paper presents that the same result can be obtained without – or modest – rescaling of the divertor transport. Reducing the additional transport stepwise to original levels in a series of simulations at first worsens the match to experiment. In particular, the density at and the ion fluxes to the inner divertor target increase to large values. However, with increasing density strong volumetric recombination starts to set in at the inner strikepoint and subsequently broadens along the target. It reduces the density at the inner target plate as well as the ion flux dramatically and brings the simulated target profiles back to experimental levels. The recombination sink rate is then comparable to the total recycling flux from all grid boundaries. This is a step forward in simulating ASDEX Upgrade H-modes as significant volumetric recombination had not been present in previous simulations of the fluctuating detachment state [8] in contrast to spectroscopic signatures of recombination in the inner divertor [9]. In addition, the results indicate that it might not be necessary to invoke additional physics, e.g. in Ref. [23], to reconcile modeling with experiment.

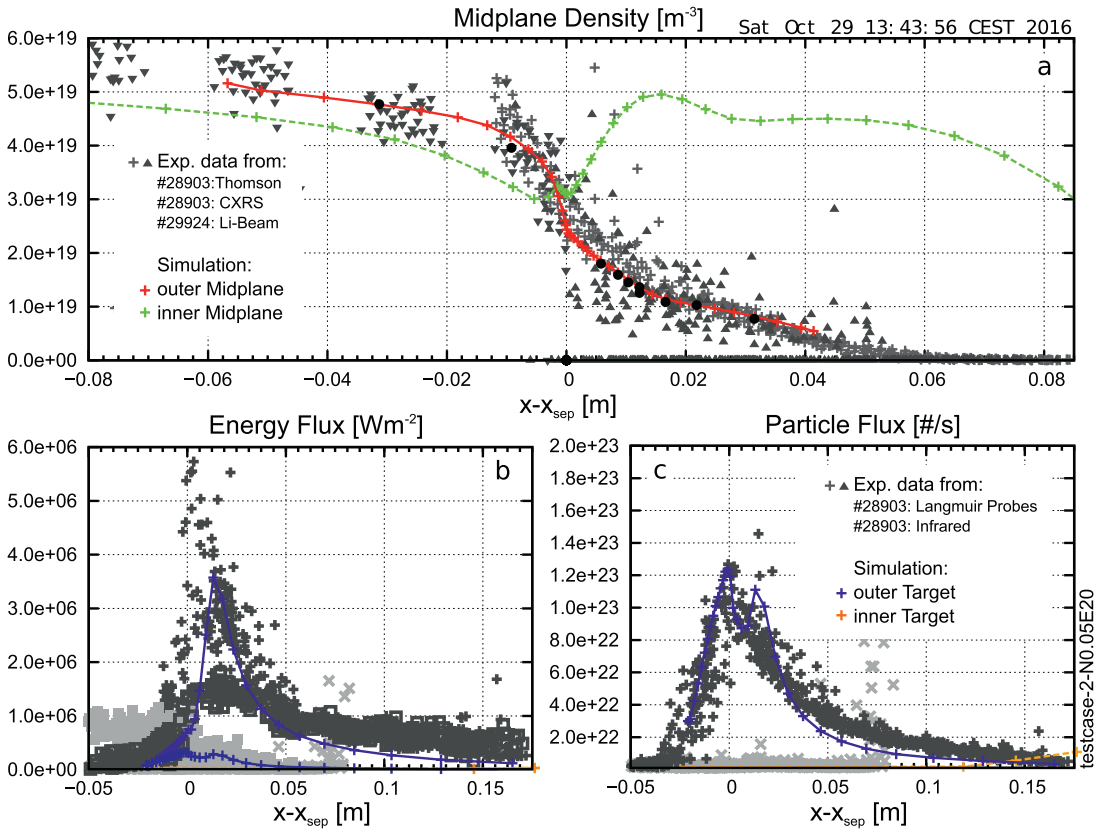

Fig. 2. a) The electron density profiles at the outer (red) and inner (green) midplane are shown along with experimental data at the outer midplane (grey). A clear in-out asymmetry of the scrape-off layer profiles and inverted gradients at the inner midplane separatrix can be seen. b) Heat flux profiles are compared to Langmuir probe and infrared thermography measurements. c) Particle flux are compared to Langmuir probe j_{sat} profiles. (For interpretation of the references to colour in this figure legend, the reader is referred to the web version of this article.)

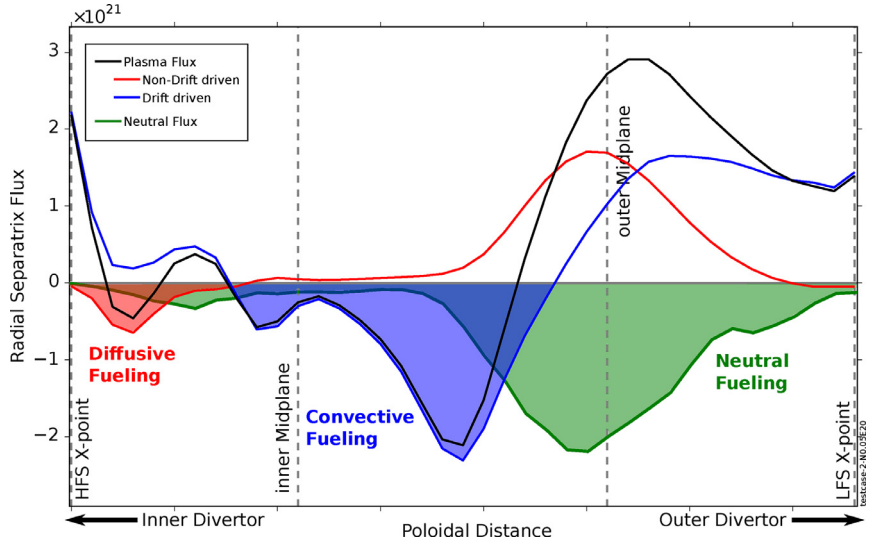

Fig. 3. The particle flux across the separatrix is plotted along the poloidal direction from X-point to X-point. The neutral fueling of the confined plasma (green) is supplemented by plasma flow driven by drifts (blue) and diffusion due to inverted density gradients (red). (For interpretation of the references to colour in this figure legend, the reader is referred to the web version of this article.)

The volumetric recombination in the simulations was triggered mainly by the increase of the density in the divertor and less so by a decrease in temperatures. This indicates the importance of three-body recombination. It is yet to be evaluated to which extent increased losses (radiation, charge-exchange, ionization) due to increased neutral density in the divertor or a change in the flow pattern are important. The neutral particle source from volumetric recombination sustains the high neutral pressure in the subdivertor without the need of large recycling fluxes from the target surface, which allows for high neutral divertor pressures and low inner target ion fluxes at experimentally observed upstream separatrix electron densities. High electron density with ionizing temperatures (>10 eV) towards the core plasma are responsible for a high opacity for neutrals towards the confined plasma. In contrast,

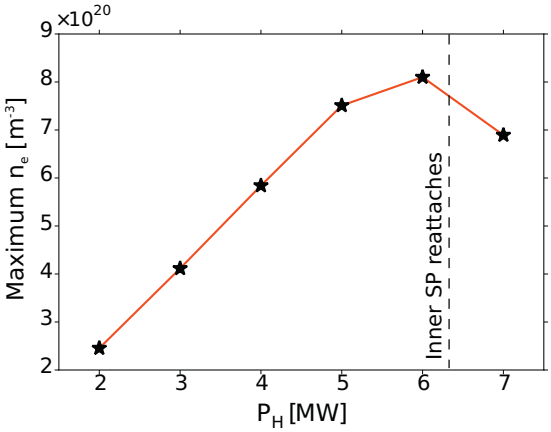

Fig. 4. Consistent with experiment, the maximum density in the high field side high densityshows a linear dependence on the heating power up to a point where the inner target starts to re-attach.

decreasing density and temperature towards the private flux region allow the neutrals to migrate from the high density region to the subdivertor volume. Both effects combined result in high neutral subdivertor pressure and high neutral compression. It is to be noted that non-drift simulations have a significantly lower peak density in the inner divertor. The high density also has a tendency to peel off the inner target and move from the divertor nose towards the X-point. A concomitant flattening of the electron density profile and a reduction of the density below the divertor nose prevents access to a state with significant recombination sinks in the inner divertor for these simulations.

4.4. The impact of impurity seeding & heating power

Experiments have shown that the high field side high densityis diminished in its spatial dimensions and its magnitude with nitrogen seeding [12]. If the nitrogen influx is increased in the simulation, the same trend is observed. First, a reduction of the density along with significantly increased radiation in the high field side scrape-off layer is observed. Concomitant with the reduction of the high field side high densitya reduced influx of plasma into the confined region and hence a drop of the separatrix density is observed. This is reminiscent of experimental observations that are connected to confinement improvement with the application of nitrogen seeding [12,13]. In the initial phase of seeding, temperatures at the outer divertor can even increase in the simulations despite the increased impurity content as the upstream density drops. The maximum target temperature then varies only slightly (∼10%) with increased seeding until the density in the inner divertor stabilizes again. At this point the outer divertor temperature starts to drop with further increased seeding and the radiation and ionization fronts move towards the X-point to ultimately form the X-point radiation with completely detached targets. The reduction of the high field side high densitywith increased nitrogen seeding is accompanied by a reduction of power into the region of strong ionization as well as a reduction of the ionization source strength in the high field side scrape-off layer. This indicates that the ionization in the inner divertor is limited by the available energy for ionization and that impurity radiation leads to a power-starvation of the recycling process, i.e. the ionization source decreases due to power balance constraints [24,25]. Simulations with a variation of the applied heating power are also in line with experimental observations and support this interpretation. Fig. 4 shows a linear variation of the maximum density in the high field side high densityregion with the heating power up to a point where the inner strikepoint temperature starts to increase and the inner divertor starts to re-attach. The linear increase of the density with heating power is consistent with experimental evidence presented in [12]. However, in ASDEX UpgradeH-mode experiments the inner divertor is usually always detached and the roll-over of the density with re-attachment of the inner target has not been observed so far. The details of the parametric dependences and the applicable parameter ranges need to be evaluated further and in greater depth in the future.

5. Discussion & summary

This contribution shows the importance of a decent match with experimental data from the high field side scrape-off layer in validated modeling of ASDEX UpgradeH-mode simulations. It is essential to match the low field side *and* high field side scrape-off layer and divertor plasma *simultaneously*. In particular, the high field side high densityis an essential contributor to the overall plasma solution. It is responsible for changes in the fueling of the confined plasma, the distribution of the neutral particle sources and the achievable neutral compression of the divertor. Drifts play a crucial role in the presented simulations in forward toroidal field ($\nabla\vec{B}$-drift pointing down). They determine the spatial extent as well as the radial and poloidal gradients of the high field side high density. In simulations with activated drift terms, inverted radial density profiles on the high field side and significant particle fluxes driven by drifts lead to plasma flow into the confined plasma. Taking into account this plasma flow in the analysis of the fueling of the confined plasma properly has enabled us to get rid of a long-standing discrepancy in the neutral compression ratio of modeling and experiment. Adapted perpendicular diffusive transport coefficients and/or the application of a convective transport component are able to reconcile the modeled neutral compression ratio with experimental values and allow to increase the divertor neutral density to experimental levels in the presented simulations – along with neutral radiation levels, the deuterium fueling rates and the measured electron densities in the inner divertor volume. In combination with the onset of strong recombination in the inner divertor this allows to drop the increased perpendicular transport in the divertor that has previously been necessary in our simulations in order to reduce the ion flux to the inner target.

In future work the applicability of the presented results to modeling of other tokamaks needs to be tested. Experimental studies [10] and initial results from our modeling of JET indicate that the existence of a high field side high densityis not restricted to ASDEX Upgrade. Detailed validation of these simulations with experimental data is still pending. For ASDEX Upgrade initial simulation results for H-Mode discharges of different heating power and fueling rates indicate that the presented discussion seems to be hold for a wider variety of plasma scenarios in ASDEX Upgrade.

Acknowledgements

The author wants to thank B. Lipschultz for fruitful discussions and suggestions on how to make the material more accessible. This work has been carried out within the framework of the EUROfusion Consortium and has received funding from the Euratom research and training program 2014–2018 under grant agreement No 633053. The views and opinions expressed herein do not necessarily reflect those of the European Commission. This work has received funding under the 2015–18 EUROfusion Researcher Grants.

Appendix A. Modeling Setup

The presented simulations are based on nitrogen seeded, medium heating power ($P_{Heat}/R = 5$ MWm^{-1}) H-mode discharges in ASDEX Upgrade [5,8]. In this study we limit ourselves to the

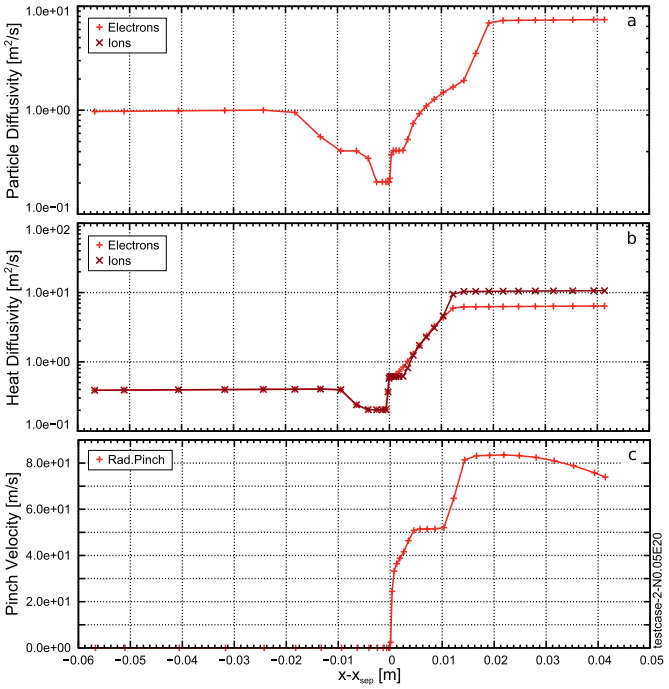

Fig. A1. The transport coefficients are shown: a) particle diffusivity, b) heat diffusivity, c) particle pinch velocity.

fluctuating detachment state. The perpendicular transport coefficient profiles at the outer midplane are shown in Fig. A.5. Identical transport coefficients are assumed for main and impurity ions. To account for the ballooning nature of transport the coefficients are rescaled in the poloidal plane by $B^2_{t,ref}/B^2_t$, where $B_{t,\,ref}$ is the average toroidal magnetic field in the simulations domain and B_t is the local toroidal magnetic field. In the outer common flux region below the X-point the transport coefficients are increased by a factor of two. In the private flux region the transport coefficients are taken to be constant with $D = 2\chi_e = 2\chi_i = 1\ \mathrm{m}^2/\mathrm{s}$. All drift terms and currents are activated in the simulations.

Fall-off lengths for the electron and ion temperature $\lambda_T = 1.0$ cm and the density $\lambda_n = 1.0$ cm and a zero perpendicular shear condition for the Mach number were used as boundary conditions at the main chamber grid boundary. At the private-flux grid boundary $\lambda_T = 1.0$ cm, $\lambda_n = 0.25$ cm and a zero perpendicular shear condition for the Mach number were set. At the targets standard sheath boundary conditions with $\gamma_e = 3.0$ and $\gamma_i = 5.0$ for the heat flux, $v_\parallel \geq c_s$ for the parallel velocity and a zero parallel gradient for the density were employed. At the core grid boundary the heat flux into electrons and ions was specified to be equal with $P_{Heat,e/i} = 2.5$ MW. The particle flux across the core boundary was chosen to be zero for all species except for deuterium, which accounts for the net influx of $8.5 \times 10^{20}\ \mathrm{s}^{-1}$ due to NBI heating. A zero perpendicular gradient of the parallel velocity $v_\parallel$ was specified. The neutral atomic data model employed is similar to Ref. [26]. The neutral domain model is calibrated to mimic the neutral conductances of the subdivertor structure [8,27,28] and a pumping speed of $S_{pump} = 114\ \mathrm{m}^3/\mathrm{s}$ of the ASDEX Upgrade pumps [29]. The recycling coefficient for all ions is taken to be 1.0 (fully recycling) at all surfaces except for the pump surfaces, where all particles are pumped with the same efficiency. At the cryopump surface the albedo is 0.81 and at the entrance to the pumping duct towards the turbopumps the albedo is 0.993.

In this work, the above described reference simulation was set up with a deuterium fueling rate of 2.0×10^{22}atoms/s. The deuterium fueling is mimicked by a gas puff of deuterium molecules at the center of the divertor dome baffle, where the divertor valves in ASDEX Upgrade are located.

References

[1] M. Shimada, D.J. Campbell, V. Mukhovatov, M. Fujiwara, N. Kirneva, K. Lackner, M. Nagami, V. Pustovitov, N. Uckan, J. Wesley, N. Asakura, A. Costley, A. Donné, E. Doyle, A. Fasoli, C. Gormezano, Y. Gribov, O. Gruber, T. Hender, W. Houlberg, S. Ide, Y. Kamada, A. Leonard, B. Lipschultz, A. Loarte, K. Miyamoto, V. Mukhovatov, T. Osborne, A. Polevoi, A. Sips, Chapter 1: overview and summary, Nucl. Fusion 47 (6) (2007) S1–S17, doi:10.1088/0029-5515/47/6/S01.

[2] P. Batistoni, Report of the Ad hoc Group on DEMO Activities, Technical Report CCE-FU 49/6., 2010.

[3] A. Loarte, B. Lipschultz, A. Kukushkin, G. Matthews, P. Stangeby, N. Asakura, G. Counsell, G. Federici, A. Kallenbach, K. Krieger, A. Mahdavi, V. Philipps, D. Reiter, J. Roth, J. Strachan, D. Whyte, R. Doerner, T. Eich, W. Fundamenski, A. Herrmann, M. Fenstermacher, P. Ghendrih, M. Groth, A. Kirschner, S. Konoshima, B. LaBombard, P. Lang, A. Leonard, P. Monier-Garbet, R. Neu, H. Pacher, B. Pegourie, R. Pitts, S. Takamura, J. Terry, E. Tsitrone, t.I.S.-o.L. Group, Diver, Chapter 4: power and particle control, Nucl. Fusion 47 (6) (2007) S203–S263, doi:10.1088/0029-5515/47/6/S04.

[4] A. Kallenbach, M. Bernert, R. Dux, L. Casali, T. Eich, L. Giannone, A. Herrmann, R. McDermott, A. Mlynek, H.W. Müller, F. Reimold, J. Schweinzer, M. Sertoli, G. Tardini, W. Treutterer, E. Viezzer, R. Wenninger, M. Wischmeier, the ASDEX Upgrade Team, Impurity seeding for tokamak power exhaust: from present devices via ITER to DEMO, Plasma Phys. Contr. Fusion 55 (12) (2013) 124041, doi:10.1088/0741-3335/55/12/124041.

[5] F. Reimold, M. Wischmeier, M. Bernert, S. Potzel, A. Kallenbach, H.W. Müller, B. Sieglin, U. Stroth, the ASDEX Upgrade Team, Divertor studies in nitrogen induced completely detached H-modes in full tungsten ASDEX Upgrade, Nucl. Fusion 55 (3) (2015) 033004, doi:10.1088/0029-5515/55/3/033004.

[6] M. Bernert, Power exhaust by SOL and pedestal radiation at ASDEX Upgrade and JET, Nucl. Mater. Energy submitted (2016).

[7] S. Potzel, M. Wischmeier, M. Bernert, R. Dux, H.W. Müller, A. Scarabosio, the ASDEX Upgrade Team, A new experimental classification of divertor detachment in ASDEX Upgrade, Nucl. Fusion 54 (1) (2014) 013001, doi:10.1088/0029-5515/54/1/013001.

[8] F. Reimold, M. Wischmeier, M. Bernert, S. Potzel, D. Coster, X. Bonnin, D. Reiter, G. Meisl, A. Kallenbach, L. Aho-Mantila, U. Stroth, Experimental studies and modeling of complete H-mode divertor detachment in ASDEX Upgrade, J. Nucl. Mater. 463 (2015) 128–134, doi:10.1016/j.jnucmat.2014.12.019.

[9] F. Reimold, M. Bernert, A. Kallenbach, B. Lipschultz, G. Meisl, S. Potzel, M.L. Reinke, M. Wischmeier, D. Wünderlich, The X-point radiation regime in detached H-Modes in full-tungsten ASDEX Upgrade, EPS 2015, Lisbon, Portugal, 2015.

[10] S. Potzel, M. Wischmeier, M. Bernert, R. Dux, F. Reimold, A. Scarabosio, S. Brezinsek, M. Clever, A. Huber, A. Meigs, M. Stamp, Formation of the high density front in the inner far SOL at ASDEX Upgrade and JET, J. Nucl. Mater. 463 (2015) 541–545, doi:10.1016/j.jnucmat.2014.12.008.

[11] L. Guimarais, V. Nikolaeva, S. Potzel, F. Reimold, M. Bernert, D. Carralero, G.D. Conway, M.E. Manso, J. Santos, A. Silva, others, LFS/HFS edge density profile dynamics on ASDEX-Upgrade, EPS 2015, European Physical Society, 2015.

[12] S. Potzel, M. Dunne, R. Dux, L. Guimarais, F. Reimold, A. Scarabosio, M. Wischmeier, On the high density in the HFS far SOL at ASDEX Upgrade and its impact on plasma confinemen, EPS 2015, Lisbon, Portugal, 2015.

[13] M.G. Dunne, Predictive modelling of the impact of a radiative divertor on pedestal confinement on ASDEX Upgrade, APS 2016, Savannah, Ohio, 2016.

[14] R. Schneider, X. Bonnin, K. Borrass, D.P. Coster, H. Kastelewicz, D. Reiter, V.A. Rozhansky, B.J. Braams, Plasma edge physics with B2-Eirene, Contrib. Plasma Phys. 46 (1–2) (2006) 3–191, doi:10.1002/ctpp.200610001.

[15] B.J. Braams, A Multi-Fluid Code for the Simulation of the Edge Plasma in Tokamaks, NET-Report 142/83-11/FU-NL/NET, 1987. Princeton, USA.

[16] D. Reiter, M. Baelmans, P. Borner, The eirene and B 2-eirene codes, Fusion Sci. Technol. 47 (2) (2005) 172–186.

[17] S. Potzel, R. Dux, H.W. Müller, A. Scarabosio, M. Wischmeier, A.U. Team, Electron density determination in the divertor volume of ASDEX Upgrade via Stark broadening of the Balmer lines, Plasma Phys. Control. Fusion 56 (2) (2014) 025010, doi:10.1088/0741-3335/56/2/025010.

[18] A. Herrmann, W. Junker, K. Gunther, S. Bosch, M. Kaufmann, J. Neuhauser, G. Pautasso, T. Richter, R. Schneider, Energy flux to the ASDEX-Upgrade diverter plates determined by thermography and calorimetry, Plasma Phys. Control. Fusion 37 (1) (1995) 17, doi:10.1088/0741-3335/37/1/002.

[19] A. Herrmann, C. Fuchs, V. Rohde, M. Weinlich, Heat flux distribution in the divertor-II of ASDEX Upgrade, J. Nucl. Mater. 266–269 (0) (1999) 291–295, doi:10.1016/S0022-3115(98)00531-5.

[20] T.D. Rognlien, G.D. Porter, D.D. Ryutov, Influence of EB and ∇B drift terms in 2-D edge/SOL transport simulations, J. Nucl. Mater. 266–269 (1999) 654–659, doi:10.1016/S0022-3115(98)00835-6.

[21] L. Aho-Mantila, On the role of drifts in the divertor power load distribution in ASDEX Upgrade, EPS 2014, Berlin, 2014.

[22] F. Reimold, Experimental Studies and Modeling of Divertor Plasma Detachment in H-Mode Discharges in the ASDEX Upgrade Tokamak, Technical University Munich, Munich, Germany, 2015 Ph.D. thesis.

[23] D. Coster, Detachment physics in SOLPS simulations, J. Nucl. Mater. 415 (1) (2011) S545–S548, doi:10.1016/j.jnucmat.2010.12.223.

[24] S.I. Krasheninnikov, A.Y. Pigarov, D.A. Knoll, B. LaBombard, B. Lipschultz, D.J. Sigmar, T.K. Soboleva, J.L. Terry, F. Wising, Plasma recombination and molecular effects in tokamak divertors and divertor simulators, Phys. Plasmas 4 (5) (1997) 1638–1646, doi:10.1063/1.872268.
[25] B. Lipschultz, J.L. Terry, C. Boswell, S.I. Krasheninnikov, B. LaBombard, D.A. Pappas, Recombination and ion loss in C-Mod detached divertor discharges, J. Nucl. Mater. 266–269 (1999) 370–375, doi:10.1016/S0022-3115(98)00534-0.
[26] V. Kotov, D. Reiter, R.A. Pitts, S. Jachmich, A. Huber, D.P. Coster, J.-E. Contributors, Numerical modelling of high density JET divertor plasma with the SOLPS4.2 (B2-EIRENE) code, Plasma Phys. Control. Fusion 50 (10) (2008) 105012, doi:10.1088/0741-3335/50/10/105012.
[27] A. Scarabosio, G. Haas, H.W. Müller, R. Pugno, M. Wischmeier, Measurements of neutral gas fluxes under different plasma and divertor regimes in ASDEX Upgrade, J. Nucl. Mater. 390–391 (2009) 494–497, doi:10.1016/j.jnucmat.2009.01.057.
[28] M. Wischmeier, X. Bonnin, D.P. Coster, A.V. Chankin, A. Kallenbach, H.W. Müller, ASDEX Upgrade Team, Simulating the role of intrinsic carbon impurities in the divertor detachment of ASDEX Upgrade, Contrib. Plasma Phys. 48 (1–3) (2008) 249–254, doi:10.1002/ctpp.200810043.
[29] B. Streibl, S. Deschka, O. Gruber, B. Jüttner, P. Lang, K. Mattes, G. Pautasso, J. Perchermeier, K. Schippl, H. Schneider, U. Seidel, W. Suttrop, G. Teller, M. Weissgerber, In-vessel cryo pump for ASDEX Upgrade divertor II, in: C. VARANDAS, F. SERRA (Eds.), Fusion Technology 1996, Elsevier, Oxford, 1997, pp. 427–430.